ELSEVIER

Journal of Contaminant Hydrology 22 (1996) 189–202

JOURNAL OF
Contaminant
Hydrology

Diffusive transport through compacted Na- and Ca-bentonite

J.-W. Choi [a], D.W. Oscarson [b,*]

[a] *Korea Atomic Energy Research Institute, Daejeon 305-353, South Korea*
[b] *AECL, Whiteshell Laboratories, Pinawa, Manitoba R0E 1L0, Canada*

Received 5 September 1994; accepted 14 July 1995

Abstract

The effect of exchangeable cation — Na^+ and Ca^{2+} — on the diffusive transport of I^-, Sr^{2+} and ^3H (as HTO) in compacted bentonite was examined using a through-diffusion method. Total intrinsic diffusion coefficients, D_i, were determined from the steady-state flux of the diffusants through the clays, and apparent diffusion coefficients, D_a, were obtained from the time lag technique. The clays were compacted to a dry bulk density of 1.3 Mg/m^3, and Na-bentonite was saturated with a solution of 100 mol $NaCl/m^3$ and Ca-bentonite with one of 50 mol $CaCl_2/m^3$. The D_i values for all diffusants are 2 to 6 times higher in the Ca- than Na-clay. We attribute this to the larger quasicrystal, or particle, size of Ca- compared to Na-bentonite. Hence, Ca-bentonite has a greater proportion of relatively large pores; this was confirmed by Hg intrusion porosimetry. This means the diffusion pathways in Ca-bentonite are less tortuous than those in Na-bentonite. Moreover, in some cases the effective porosity, or the porosity available for diffusive transport, may be greater in Ca-bentonite. The D_a values are inversely proportional to the distribution coefficients of the diffusants with the clays.

1. Introduction

Bentonite-based materials are being evaluated in several countries as potential barriers and seals in a disposal vault for nuclear fuel waste. In both Canada and Korea, for example, compacted bentonite-based materials would be used in a vault to surround containers holding nuclear fuel waste (Choi et al., 1991; Hancox and Nuttall, 1991). Because of the low permeability of compacted bentonite, diffusion is the principal mechanism of mass transport through these barriers.

* Corresponding author.

SSDI 0169-7722(95)00081-X

The nature of the cation on the exchange complex of bentonite (or, more properly, montmorillonite, the principal component of bentonite) greatly affects many of its properties, including its swelling potential, permeability and diffusivity (Dutt and Low, 1962; Mesri and Olson, 1971; Yong and Warkentin, 1975; Shainberg et al., 1988). Here we examine the effect of the exchangeable cation — Na^+ and Ca^{2+} — on the diffusive properties of compacted Avonlea bentonite. This clay is a component of the reference buffer material in the disposal concept developed in Canada for nuclear fuel waste.

The cation exchange complex of untreated Avonlea bentonite contains ~ 60% Na^+ and ~ 20% Ca^{2+}, along with minor amounts of Mg^{2+} and K^+. However, as groundwater slowly moves through the bentonite in a disposal vault, Ca^{2+} will gradually become the main exchangeable cation. This is because its concentration is generally greater than that of Na^+ in deep groundwaters of the Canadian Shield where a vault would be located (Frape et al., 1984); and the selectivity coefficient is > 1 for $Na^+ \rightarrow Ca^{2+}$ exchange on bentonite (Benson, 1982). Besides Ca^{2+} in groundwater, it may also be released from cement grouts that could be used in a vault. Since, initially, Na^+ will be the main exchangeable cation associated with bentonite in a vault, but will be progressively replaced by Ca^{2+}, it is important to evaluate the diffusive behaviour of both Na- and Ca-bentonite.

An anion (I^-), a cation (Sr^{2+}) and a neutral species (^3H, as HTO) were used as diffusants. Iodine-129 is an important radioisotope in nuclear fuel waste management due to its long half-life (1.6×10^7 a) and because it does not strongly sorb on earthen materials like clays and rocks. Although $^{90}Sr^{2+}$ is not particularly important with respect to long-term disposal of nuclear fuel waste because of its relatively short half-life of 29 a, its chemistry is comparatively simple, and it can therefore serve as a model for the behaviour of cations in compacted clay. And the migration behaviour of HTO, a small, non-sorbing species, can provide important information on the pore structure of compacted clay.

2. Experimental

2.1. Clay

The Avonlea bentonite is from the Bearpaw Formation of Late Cretaceous age in southern Saskatchewan, Canada. The clay contains ~ 80 wt% smectite (montmorillonite), ~ 10 wt% illite, ~ 5 wt% quartz, and minor amounts of gypsum, feldspar and carbonate (Oscarson and Dixon, 1989). It has a cation-exchange capacity of ~ 60 $cmol_c/kg$ and a specific surface area of 480×10^3 m^2/kg.

The reference buffer material in the Canadian disposal concept is a 1:1 mix by dry mass of Avonlea bentonite and silica sand compacted to a dry bulk density of ~ 1.7 Mg/m^3. With respect to diffusion and sorption processes, however, clay is the active component of the buffer and sand is essentially inert filler provided the clay content of the mix is greater than ~ 20 wt.% (Gillham et al., 1984; Sharma and Oscarson, 1991). Hence, 100% clay was used in this study.

To saturate the clay's exchange complex with Na^+ or Ca^{2+}, 100 g of bentonite were washed several times with 500 cm^3 of a 1000 mol/m^3 solution of NaCl or $CaCl_2$. The Na- and Ca-clays were dialyzed against deionized water for several days to remove excess salt, and then freeze-dried. The clays were compacted to a target dry bulk density, ρ, of 1.3 Mg/m^3 in stainless-steel rings (4.1 cm in diameter and 0.7 cm long) using a hydraulic press. The same rings and compacting procedure were used for both the porosity measurements and the diffusion experiments described below. A density of 1.3 Mg/m^3 is close to the effective clay density of a 1:1 mix of clay and sand compacted to 1.7 Mg/m^3. (Effective clay density is the ratio of the mass of dry clay to the combined volume of clay and pores.)

2.2. Hg intrusion porosimetry

Pore parameters of compacted Na- and Ca-bentonite were obtained as follows. The compacted clays in the steel rings were sandwiched between porous Ni discs and constrained in specially-designed stainless-steel holders. The plugs were immersed in a solution of either 100 mol $NaCl/m^3$ or 50 mol $CaCl_2/m^3$ for ~ 4 weeks. From previous experiments, this is enough time to saturate the compacted clays. The plugs were then slowly dried — to minimize disruption of the pore structure — in chambers having progressively drier atmospheres. The relative humidities (over H_2SO_4 solutions) in the chambers were 81%, 58% and 3.2%. The plugs were kept at a given humidity for at least 2 weeks. The clays were then examined by Hg intrusion porosimetry to 414 MPa. At the maximum intrusion pressure of 414 MPa, Hg can theoretically enter pores with a diameter as small as 3.6 nm. Before the measurement, the samples were outgassed at 6.5 Pa at room temperature.

2.3. Diffusion experiments

A diagram of the diffusion cell is shown in Fig. 1, and it is described by Hume (1993). The through-diffusion experiments, conducted in triplicate at $23 \pm 2°C$, are described in detail by Oscarson et al. (1992). Briefly, the experiment involves flowing a solution containing a diffusant (^{125}I, ^{85}Sr, or ^{3}H in this study; some properties of these radioisotopes are given in Table 1) from a source reservoir over one end of a clay plug and passing an unspiked solution from a collection reservoir over the other end. The diffusant then moves through the plug under a concentration gradient. The background

Table 1
Selected properties of the radiosiotopes

Radioisotope	Half-life	Specific activity (PBq/mol)	D_o [a] ($\mu m^2/s$)	r_H [b] (nm)
^{125}I	60.2 d	80.3	1940	0.33
^{85}Sr	64.8 d	74.6	757	0.41
^{3}H (HTO)	12.3 a	1.08	2450	0.14

[a] Diffusion coefficient in pure bulk water under stationary conditions; values for I and Sr from Li and Gregory (1974) and HTO from McCall and Douglass (1965).
[b] Effective hydrated radius (Nightingale, 1959).

solution in both the source and collection reservoirs was either 100 mol $NaCl/m^3$ or 50 mol $CaCl_2/m^3$; the clays were also saturated with these solutions before starting the diffusion experiments. The concentration of HTO in the source reservoir was 15 $\mu mol/m^3$; for I and Sr, stable isotope was added as a carrier and their total concentration in the source reservoir was $\sim$ 1 $mmol/m^3$. The activity in the source reservoir was monitored by liquid scintillation counting. When it decreased to 90% of the starting activity, diffusant was added to bring its concentration up to that of the original solution. In this way, the diffusant concentration in the source reservoir was kept nearly constant throughout a run. The flow rate of the solution over the outflow end of the clay plugs was such that when a diffusant passed through the plug, it was quickly "swept away". Hence, at the outflow end of the plug the diffusant concentration was always close to zero.

The flux of a diffusant through the clay plugs was measured with time and when steady-state was established, total intrinsic diffusion coefficients, D_i (also called effective diffusion coefficients by many investigators), were calculated from a form of Fick's first law:

$$J = -D_i\left(\frac{dc}{dx}\right) \tag{1}$$

as

$$D_i = -J\Big/\left(\frac{dc}{dx}\right) = -\left(\frac{\Delta Q}{A\Delta t}\right)\Big/\left(\frac{\Delta c}{L}\right) \tag{2}$$

where J is the diffusant flux; Q the cumulative amount of diffusant passing through the clay plug; ΔQ the amount passing through in an increment of time Δt; A the cross-sectional area; L the length of the plug; and Δc the difference in the diffusant concentration between the ends of the plug. Since solutions were allowed to flow through porous discs next to the plug (Fig. 1), the concentration of the diffusant was assumed to be equal to the concentration in the source reservoir, c_o, at one end of the plug and zero at the other end. The use of difference operators in Eq. 2 implies a linear diffusant concentration through the clay plugs; this is the case in these experiments as shown elsewhere (Oscarson et al., 1992; Cho et al., 1993).

If aqueous phase diffusion is the only mechanism of diffusive transport, $D_i = D_{iw}$, where D_{iw} is the intrinsic diffusion coefficient in pore water and is given as:

$$D_{iw} = D_o\psi = D_o\tau n_e \tag{3}$$

where D_o is the diffusion coefficient in pore bulk water under stationary conditions; Ψ the diffusibility of the porous medium; τ the tortuosity factor; and n_e the effective porosity or the porosity available for diffusive transport.

The tortuosity factor is usually expressed as:

$$\tau = \left(\frac{L}{L_e}\right)^2 \tag{4}$$

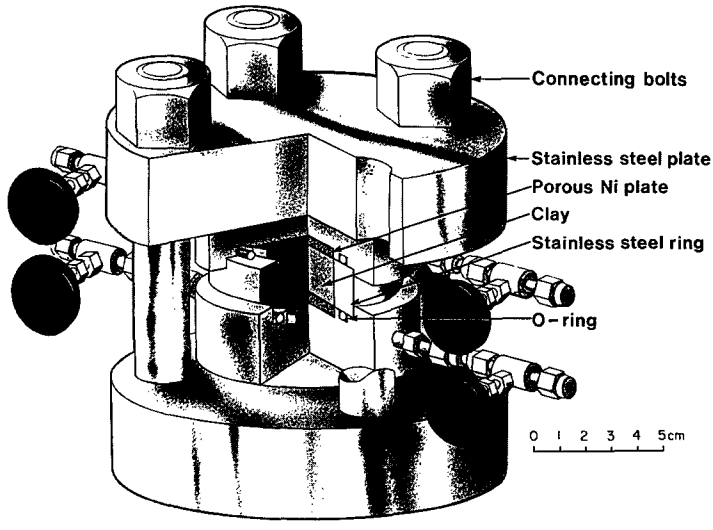

Fig. 1. Diagram of the diffusion cell.

where L is the straight-line macroscopic distance between two points defining the transport path, and L_e is the actual, microscopic or effective distance between the same two points. Since $L_e > L$ for porous media, $\tau < 1$. In reality, τ may account for more than just the pore geometry of the clay. Another factor that may be included in τ is, for instance, the variation in the viscosity of the solution within the pore space (Kemper et al., 1964).

From these experiments, another diffusion coefficient, an apparent diffusion coefficient, D_a, can be determined from the time lag, t_e. The t_e value is obtained by extrapolating from the steady-state region of cumulative flux curves to the time axis. For this experiment the solution to Fick's second law, expressed by the following equation,

$$\frac{\partial c'}{\partial t} = D_a \frac{\partial^2 c'}{\partial x^2} \tag{5}$$

is (Crank, 1975):

$$\frac{Q}{ALc_o'} = \frac{D_a t}{L^2} - \frac{1}{6} - \frac{2}{\pi^2} \sum_{n=1}^{n=\infty} \frac{(-1)^n}{n^2} \exp\left(\frac{-D_a n^2 \pi^2 t}{L^2} \right) \tag{6}$$

which, as $t \to \infty$, approaches the line,

$$\frac{Q}{A} = \frac{D_a c_o'}{L} \left(t - \frac{L^2}{6D_a} \right) \tag{7}$$

The intercept of the slope at the t-axis ($Q/A = 0$) gives t_e, which is related to D_a by:

$$D_a = \frac{L^2}{6t_e} \tag{8}$$

Eq. 6 is subject to the following initial and boundary conditions:

$$c'(0 < x \leq L, 0) = 0$$

and

$$c'(0,t) = c'_o, \quad c'(L,t) \ll c'_o$$

where $c' = c\alpha$; $c'_o = c_o\alpha$, which is the initial bulk concentration of the diffusant in the clay immediately next to the source reservoir; and α is the capacity factor (the capacity of the solution and solid per unit volume of the bulk porous medium to hold more of the diffusant as its concentration in the solution phase increases by one unit).

The D_a value is defined as:

$$D_a = \frac{D_i}{\alpha} = \frac{D_o \tau n_e}{(n_e + \rho K_d)} \tag{9}$$

where ρ is the dry bulk density; and K_d the solid/solution distribution coefficient; it is given as,

$$K_d = \frac{q}{c} \tag{10}$$

where q is the amount of a diffusant associated with the clay, and c its concentration in the pore solution in local equilibrium with the clay. The use of K_d implies a linear sorption isotherm passing through the origin. This is a reasonable assumption for most sorbates or diffusants when present in low concentrations (< 1 mmol/m^3 or so) which is the case here.

2.4. Sorption experiments

The extent of sorption of I^- and Sr^{2+}, expressed as K_d, on Na- and Ca-bentonite was determined by suspending 5 g of clay in 30 cm^3 of 100 mol NaCl/m^3 or 50 mol $CaCl_2$/m^3 solution spiked with ^{125}I or ^{85}Sr in 50-cm^3 polycarbonate centrifuge tubes. Stable isotopes were added as carriers and the total concentration of I and Sr was ~ 1 mmol/m^3, the same as that in the source reservoir in the diffusion experiments. The tubes were capped, sealed in polyethylene bags, and placed in a water bath at 23 ± 0.1°C for 30 days. The tubes were shaken periodically. After the reaction period, the tubes were centrifuged at $5500g$ for 40 min. The activity of ^{125}I or ^{85}Sr in the supernatant solution was measured by liquid scintillation counting. Blank experiments, conducted identically but without clay, showed that no detectable I^- or Sr^{2+} sorbed on the centrifuge tubes. Values of K_d were calculated from:

$$K_d = \left(\frac{A_i}{A_e} - 1\right)(S - S_a)/\rho_w \tag{11}$$

where A_i is the net activity of the solution initially added to the clay; A_e the net activity of the solution after the reaction period; S the solution/clay ratio (by mass); S_a the

Table 2
Pore parameters for compacted Na- and Ca-bentonite from Hg intrusion porosimetry

	Na-bentonite	Ca-bentonite
Total intrusion volume [a] (cm^3/kg)	96.7	152
Median pore diameter [b] (nm)	12.7	24.4
Average pore diameter [c] (nm)	10.3	16.5

[a] Maximum volume of Hg intruded into the sample at the highest pressure attained during the test.
[b] 50% (percentile) values obtained from volume distribution curves.
[c] Pore volume divided by pore area ($4V/A$); assumes all pores are right cylinders.

solution/clay ratio, or gravimetric moisture content, of the air-dried clay; and ρ_w the density of the NaCl or $CaCl_2$ solutions.

3. Results and discussion

3.1. Hg intrusion porosimetry

Even though the *total* porosity of the two clays is the same at a given density, porosimetry measurements show that the pore-size distribution of the two clays is markedly different. There are more large pores in compacted Ca- than Na-bentonite: the total intrusion volume, and the median and average pore size are all greater for Ca-bentonite (Table 2). There is also a bimodal distribution of pore sizes in the Ca-bentonite (Figs. 2 and 3): one centred around a pore diameter of 0.01 μm and the other around 1 μm. The larger pores are not present in Na-bentonite. We attribute the greater proportion of large pores in Ca-bentonite to the larger quasicrystal, or particle, size of this clay compared to that of Na-bentonite.

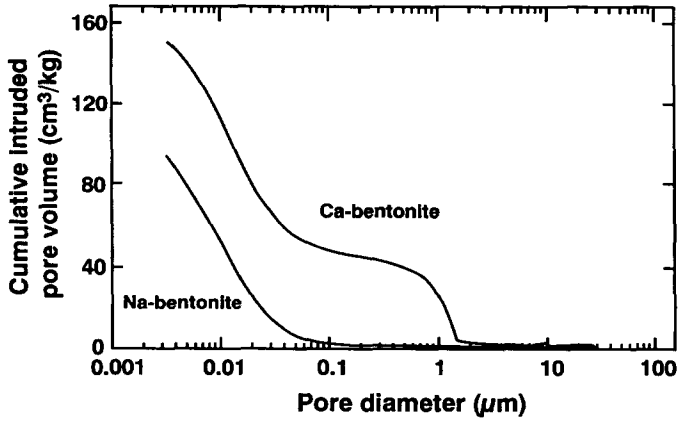

Fig. 2. Cumulative intruded pore volume vs. pore diameter of Na- and Ca-bentonite.

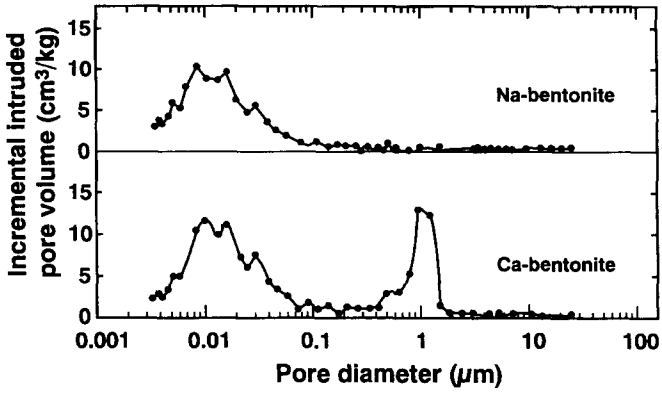

Fig. 3. Incremental intruded pore volume vs. pore diameter of Na- and Ca-bentonite.

Quasicrystals are defined as several hydrated unit layers of montmorillonite (or other smectite clays) stacked in roughly parallel alignment along the crystallographic c-axis (Quirk and Aylmore, 1971). This particle structure is stabilized by attractive interactions between the basal planes of unit layers mediated by adsorbed cations and water (Sposito, 1984). In dilute aqueous suspension, Ca-bentonite forms quasicrystals with 4 to 7 unit layers, while those of Na-bentonite are thought to average ~ 1.3 unit layers (Sposito, 1984). The quasicrystals of montmorillonite when present as a gel or paste are likely composed of a greater number of unit layers than those in dilute aqueous suspension, but the number of layers per quasicrystal of Ca-montmorillonite is still much higher than that of Na-montmorillonite. For example, Ben Rhaiem et al. (1987) reported that in a gel the number of unit layers per quasicrystal of Ca-montmorillonite ranged from 50 to 400, while that of Na-montmorillonite was ≤ 10. Our porosimetry data suggest the relative number of unit layers in a quasicrystal of Ca- and Na-bentonite is maintained when clays are freeze-dried and subsequently compacted and saturated.

We attribute the larger pores in Ca-bentonite to interparticle pores — pores between clay particles when they are packed together and that are intruded during the test, and the smaller pores to intraparticle pores — pores lying within the exterior outlines of individual clay particles. The less ordered structure of Na-bentonite allows the particles to disperse relatively uniformly throughout the available space and thus the larger, 1-μm pores in Ca-bentonite are not present in Na-bentonite (Fig. 3).

3.2. Total intrinsic diffusion coefficients

Typical cumulative flux curves for HTO through Na- and Ca-bentonite are shown in Fig. 4 and those for Sr^{2+} in Fig. 5. The curves for I^- are similar to those for untreated Avonlea bentonite given elsewhere (Oscarson et al., 1992). For all diffusants, the flux through Ca-bentonite is greater than that through Na-bentonite. Since D_i is a proportionality constant relating the flux of a diffusant to its concentration gradient (Eq. 2), and the concentration gradient for a given diffusant was the same for both clays, D_i is also

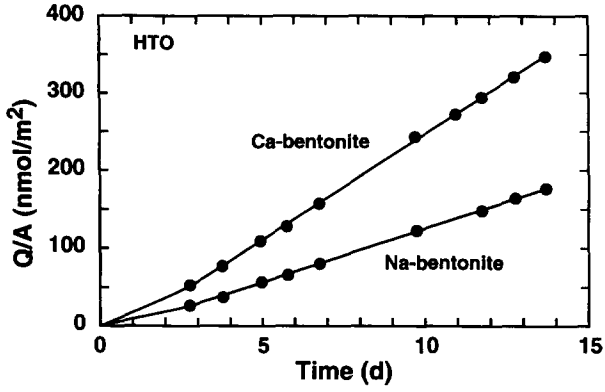

Fig. 4. Cumulative flux curves for HTO in Na- and Ca-bentonite.

greater in the Ca-bentonite. We attribute the higher D_i values in Ca-bentonite to the greater proportion of comparatively large pores in this clay and to their influence on Ψ.

The D_i values depend on D_o and Ψ (Eq. 3). For a given diffusant, D_o should be similar in the NaCl and $CaCl_2$ solutions (McCall and Douglass, 1965). From the HTO data, Ψ was estimated (Table 3) for the two clays from the ratio D_i/D_o. The higher Ψ in the Ca- than Na-bentonite suggests that τ or n_e (or both) is greater in the Ca-clay (Eq. 3). It is likely that HTO migrates through all, or nearly all, of the pore space of compacted clays (Henrion et al., 1991; Kato et al., 1995). If so, $n_e \simeq n$, the total porosity, and τ can be estimated (Table 3) from the ratio Ψ/n. (At $\rho = 1.3$ Mg/m^3, $n = 0.52$, assuming a particle density of 2.7 Mg/m^3 for both clays.) The higher τ in Ca-bentonite means the diffusion pathways in this clay are less tortuous (τ is greater, Eq. 4) than those in Na-bentonite.

The mobility of the first molecular layer of water sorbed on Na-bentonite is ~ 30% of the mobility of water molecules in bulk water, and that on Ca-bentonite, ~ 5% (Kemper et al., 1964). Therefore, D_i for HTO would be expected to be higher in

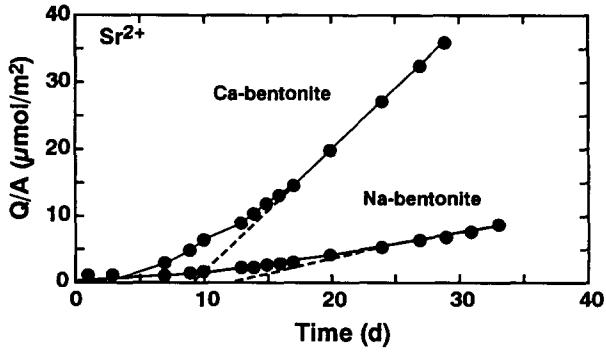

Fig. 5. Cumulative flux curves for Sr^{2+} in Na- and Ca-bentonite. The point where the *dashed lines*, extrapolated from the steady-state region of the curves, intercept the time axis gives t_e, the time lag.

Table 3
Diffusion coefficients for HTO and diffusibility and tortuosity factors in the Na- and Ca-bentonite

Clay	D_i ($\mu m^2/s$)	Ψ [a]	τ [b]	D_a ($\mu m^2/s$)
Na-bentonite	78 ± 34 [c]	0.032	0.062	80 ± 20
Ca-bentonite	150 ± 15	0.061	0.117	110 ± 16

[a] Diffusibility factor for the clays from Eq. 3 for HTO.
[b] Tortuosity factor for the clays calculated from the ratio Ψ / n_e, where n_e for HTO diffusion is assumed to equal the total porosity of the clays.
[c] Arithmetic mean $\pm$ one standard deviation of three replicates.

Na-bentonite, other factors being equal. Since the opposite is observed (Table 3), the greater proportion of large pores in Ca-bentonite, and their influence on τ, outweighs the comparatively low mobility of HTO next to particles of Ca-bentonite.

For I^-, $D_i < D_{iw}$ for both clays (Table 4); this is likely due to anion exclusion. Similar results for I^- in compacted clays have been reported by others (Berry and Bond, 1992; Oscarson, 1994). This suggests I^- migrates through less of the pore space (n_e is lower) than HTO. If so, Ψ obtained from HTO experiments is overestimated for I^-. A lower Ψ would give a proportionately lower D_{iw} (Eq. 3) for I^-, and closer to the measured D_i.

The D_i results for I^- also agree with electrical double-layer theory. The double layer of Na-bentonite is more diffuse than that of Ca-bentonite (Yong and Warkentin, 1975); thus, Na-bentonite has less pore space available for anion diffusion, i.e. a greater degree of anion exclusion. For I^- in Na-bentonite, D_i is ~ 8 times less than D_{iw}, but only 4 times less in Ca-bentonite (Table 4).

If we assume τ is a property of a porous medium only and that it does not depend on the diffusant, then an estimate of n_e for I^- can be obtained from $D_i/D_o\tau$ (Eq. 3). In Na-bentonite, $n_e = 0.06$ and in Ca-bentonite, 0.13. Therefore, not only are the diffusion pathways less tortuous in Ca-bentonite, but its effective porosity for I^- diffusion is greater than that of Na-bentonite. Again, we ascribe this to the greater proportion of large pores in Ca-bentonite. These n_e values of bentonite for I^- of ~ 0.1, or 20% of n (0.52), at $\rho = 1.3$ Mg/m^3 are similar to those reported by others (Oscarson et al., 1992; Cho et al., 1993).

Table 4
Diffusion and distribution coefficients in the clays

Clay	Diffusant	D_i ($\mu m^2/s$)	D_{iw} ($\mu m^2/s$)	D_a ($\mu m^2/s$)	calc. D_a [a] ($\mu m^2/s$)	K_d (m^3/Mg)
Na-bentonite	I	7.5 ± 0.71 [b]	62	48 ± 1.4	1.6	3.4 ± 0.23
	Sr	24 ± 16	24	8.5 ± 2.1	0.25	76 ± 3.1
Ca-bentonite	I	29 ± 15	120	16 ± 7.1	3.0	7.4 ± 0.62
	Sr	150 ± 40	45	18 ± 10	2.9	12 ± 0.0

[a] Calculated from Eq. 9.
[b] Arithmetic mean $\pm$ one standard deviation of three replicates.

For Sr^{2+}, $D_i = D_{iw}$ in Na-bentonite (Table 4), indicating that Ψ, estimated from HTO experiments, is appropriate for Sr^{2+} in this clay. On the other hand, $D_i > D_{iw}$ in Ca-bentonite. Thus, Sr^{2+} migrates through the Ca-bentonite at a rate greater than predicted from aqueous phase diffusion alone (Eq. 3). Some investigators have invoked surface diffusion, or migration within the electrical double layer next to clay surfaces, to account for enhanced diffusion of cations like Sr^{2+} in some clay–water systems (Oscarson, 1994 and references therein). If there is surface diffusion, Eq. 3 is modified to (Oscarson, 1994):

$$D_i = D_o \psi + D_s \rho K_d \tag{12}$$

where D_s is the surface diffusion coefficient. This equation predicts that D_i increases with increasing K_d. Clearly this is not the case for Sr^{2+}: K_d is lower and D_i higher in the Ca- than Na-bentonite (Table 4). Oscarson (1994) also reported enhanced diffusion of Sr^{2+} in the Avonlea bentonite at $\rho = 1.25$ Mg/m^3, but not at $\rho = 1.60$ Mg/m^3. It is not clear why there is apparently enhanced migration of Sr^{2+} in some clay–water systems, but not in others. This requires further study and perhaps more advanced models of cation migration in compacted clays.

In Avonlea bentonite at $\rho \sim 1.3$ Mg/m^3 and saturated with a synthetic groundwater solution, the mean D_i values for the three diffusants are: 12 μm^2/s for I^-, 79 μm^2/s for Sr^{2+} and 120 μm^2/s for HTO (Oscarson, 1994). All these values fall between those obtained for Na- and Ca-bentonite (Tables 3 and 4). In Oscarson's study, the synthetic groundwater solution had the following major-ion concentrations in mol/m^3: Na^+, 83; Ca^{2+}, 53; Cl^-, 170; and SO_4^{2-}, 11. This result suggests untreated Avonlea bentonite saturated with the synthetic groundwater solution (in this case the exchange complex of the clay contains both Na^+ and Ca^{2+} along with minor amounts of Mg^{2+} and K^+) has a pore structure or fabric intermediate between those of pure Na- and Ca-bentonite. A corollary is that the number of unit layers per quasicrystal of the untreated bentonite saturated with the synthetic groundwater solution is greater than that for Na-bentonite, but less than the number for Ca-bentonite. It is well known that the size of montmorillonite particles change with various cation substitutions on the clay's exchange complex (Sposito, 1984).

As Ca^{2+} gradually replaces Na^+ on the exchange complex of bentonite in a disposal vault, D_i for radioisotopes in a bentonite-based barrier would be expected to increase accordingly. The increase, though, would only be about a factor of 5, at most. Based on a sensitivity analysis of mass diffusion in clay-based barriers, this relatively small increase is not significant in the nuclear waste disposal concept developed in Canada (Johnson et al., 1994).

On the other hand, when compacted, clay layers have restricted mobility. Hence they may be unable to assume other arrangements; for example, more unit layers per quasicrystal as the proportion of Ca^{2+} on the exchange complex increases. If so, compacted clay would likely maintain the diffusivity of that initially emplaced in a disposal vault regardless of how the exchangeable cation composition evolves. Confirmation of this requires further study, but the results of Whitworth and Fritz (1994) on the permeability of compacted smectite membranes tend to support this argument.

3.3. Apparent diffusion coefficients

The t_e values, from which D_a values were determined (Eq. 8), are obtained by extrapolating from the steady-state region of cumulative flux curves to the time axis; this is shown, for example, as dashed lines in Fig. 5. From this figure, t_e for Sr^{2+} is 13.5 days in Na-bentonite and 8.8 days in Ca-bentonite. For clarity, the extrapolation is not shown for HTO in Fig. 4.

The lower D_a values for I^- and Sr^{2+} compared to HTO in both clays is largely because they sorb on the clays and HTO does not. Moreover, consistent with Eq. 9, D_a for I^- and Sr^{2+} is inversely proportional to K_d. The D_a values for I^- are lower in Ca- than Na-bentonite even though Ca-bentonite has less tortuous diffusion pathways and a greater n_e as discussed above. This illustrates the strong dependence of D_a on sorption reactions. Less Sr^{2+} is sorbed on Ca- than Na-bentonite because of greater competition from divalent Ca^{2+} than monovalent Na^+ for sorption sites on the clays (Benson, 1982).

Values of D_a calculated from Eq. 9 are given in Table 4 for comparison with the measured D_a values. The K_d values used in the calculation are also shown in Table 4. The other parameters used in Eq. 9 for I^- are: $D_o = 1940\ \mu m^2/s$; $\rho = 1.3\ Mg/m^3$; $\tau = 0.062$ (Na-bentonite) and 0.117 (Ca-bentonite); and $n_e = 0.06$ (Na-bentonite) and 0.13 (Ca-bentonite). The parameters for Sr^{2+} are: $D_o = 757\ \mu m^2/s$; $n_e = 0.52$ for both clays; and ρ and τ are the same as those for I^-.

The calculated D_a values are lower than the measured ones. We attribute this largely to an overestimation of K_d measured in batch tests on loose bentonite at a relatively high solution/clay ratio. Lower K_d values would give higher calculated D_a values (Eq. 9), and perhaps closer to the measured values. The K_d values in Table 4 likely overestimate the actual extent of sorption of a diffusant on compacted clays for at least two reasons. First, K_d generally decreases with decreasing solution/clay ratio (Meier et al., 1987; Robin et al., 1987; Oscarson et al., 1994). If K_d values could have been measured on the compacted clays where the solution/clay ratio was $\sim 0.4\ m^3/Mg$, they would likely be lower than those determined on the loose clays in the batch tests at a solution/clay ratio of 6 m^3/Mg. Secondly, at a given solution/clay ratio, K_d for sorbates on compacted bentonite are lower than those on loose bentonite (Oscarson et al., 1994). This is because sorbates cannot access all sorption sites on compacted clays.

4. Summary

We examined the effect of the exchangeable cation — Na^+ and Ca^{2+} — on the diffusive behaviour of I^-, Sr^{2+} and HTO in compacted bentonite. Total intrinsic diffusion coefficients for all diffusants are higher by a factor of 2 to 6 in Ca- than Na-bentonite. This is due to the larger particle size of Ca-bentonite, which, in turn, means there is a greater proportion of relatively large pores; this was confirmed by Hg intrusion porosimetry. Hence, the diffusion pathways in Ca-bentonite are less tortuous, and, in some cases, the effective porosity for diffusion is greater. The D_a values for the diffusants are inversely proportional to K_d.

Acknowledgements

We thank Mr. H.B. Hume for assistance with the diffusion and sorption experiments, and Mr. B.T. Walker for conducting the Hg intrusion porosimetry. The Canadian Nuclear Fuel Waste Management Program is funded jointly by AECL and Ontario Hydro under the auspices of the CANDU Owners Group.

References

Ben Rhaiem, H., Pons, C.H. and Tessier, D., 1987. Factors affecting the microstructure of smectites: Role of cation and history of applied stresses. In: L.G. Schultz, H. van Olphen and F.A. Mumpton (Editors), Proceedings of International Clay Conference, Denver, 1985. Clay Miner. Soc., Bloomington, IN, pp. 292–297.

Benson, L.V., 1982. A tabulation and evaluation of ion exchange data on smectites. Environ. Geol., 4: 23–29.

Berry, J.A. and Bond, K.A., 1992. Studies of the extent of surface diffusion in the migration of radionuclides through geological materials. Radiochim. Acta, 58/59: 329–335.

Cho, W.-J., Oscarson, D.W., Gray, M.N. and Cheung, S.C.H., 1993. Influence of diffusant concentration on diffusion coefficients in clay. Radiochim. Acta, 60: 159–163.

Choi, J.-W., Whang, J.-H., Chun, K.-S. and Lee, B.-H., 1991. Applicability of domestic bentonite as a buffer material of spent fuel repository. J. Korean Nucl. Soc., 23: 410–419.

Crank, J., 1975. The Mathematics of Diffusion. Oxford University Press, London, 2nd ed.

Dutt, G.R. and Low, P.F., 1962. Relationship between the activation energies for deuterium oxide diffusion and exchangeable ion conductance in clay systems. Soil Sci., 93: 195–203.

Frape, S.K., Fritz, P. and McNutt, R.H., 1984. Water–rock interaction and chemistry of groundwaters from the Canadian Shield. Geochim. Cosmochim. Acta, 48: 1617–1627.

Gillham, R.W., Robin, M.J.L., Dytynyshyn, D.J. and Johnston, H.M., 1984. Diffusion of nonreactive and reactive solutes through fine-grained barrier materials. Can. Geotech. J., 21: 541–550.

Hancox, W.T. and Nuttall, K., 1991. The Canadian approach to safe, permanent disposal of nuclear fuel waste. Nucl. Eng. Des., 129: 109–117.

Henrion, P.N., Put, M.J. and van Gompel, M., 1991. The influence of compaction on the diffusion of non-sorbed species in Boom clay. Radioact. Waste Manage. Nucl. Fuel Cycle, 16: 1–14.

Hume, H.B., 1993. Procedures and apparatus for measuring diffusion and distribution coefficients in compacted clays. AECL, Chalk River, Ont., Rep. AECL-10981, COG-93-447.

Johnson, L.H., LeNeveu, D.M., Shoesmith, D.W., Oscarson, D.W., Gray, M.N., Lemire, R.J. and Garisto, N.C., 1994. The disposal of Canada's nuclear fuel waste: The vault model for postclosure assessment. AECL, Chalk River, Ont., AECL-10714, COG-93-4.

Kato, H., Muroi, M., Yamada, N., Ishida, H. and Sato, H., 1995. Estimation of effective diffusivity in compacted bentonite. In: Scientific Basis for Nuclear Waste Management, Vol. 353. Kyoto, pp. 277–284.

Kemper, W.D., Maasland, D.E.L. and Porter, L.K., 1964. Mobility of water adjacent to mineral surfaces. Soil Sci. Soc. Am. Proc., 28: 164–167.

Li, Y.-H. and Gregory, S., 1974. Diffusion of ions in sea water and deep-sea sediments. Geochim. Cosmochim. Acta, 38: 703–714.

McCall, D.W. and Douglass, D.C., 1965. The effect of ions on the self-diffusion of water, I. Concentration dependence. J. Phys. Chem., 69: 2001–2011.

Meier, H., Zimmerhackl, E., Zeitler, G., Menge, P. and Hecker, W., 1987. Influence of liquid/solid ratio in radionuclide migration studies. J. Radioanal. Nucl. Chem., 109: 139–151.

Mesri, G. and Olson, R.E., 1971. Mechanisms controlling the permeability of clays. Clays Clay Miner., 19: 151–158.

Nightingale, Jr., E.R., 1959. Phenomenological theory of ion solvation. Effective radii of hydrated ions. J. Phys. Chem., 63: 1381–1387.

Oscarson, D.W., 1994. Surface diffusion: Is it an important transport mechanism in compacted clays? Clays Clay Miner., 42: 534–543.

Oscarson, D.W. and Dixon, D.A., 1989. Elemental, mineralogical, and pore-solution compositions of selected Canadian clays. AECL, Chalk River, Ont., Rep. AECL-9891.

Oscarson, D.W., Hume, H.B., Sawatsky, N.G. and Cheung, S.C.H., 1992. Diffusion of iodide in compacted bentonite. Soil Sci. Soc. Am. J., 56: 1400–1406.

Oscarson, D.W., Hume, H.B. and King, F., 1994. Sorption of cesium on compacted bentonite. Clays Clay Miner., 42: 731–736.

Quirk, J.P. and Aylmore, L.A.G., 1971. Domains and quasi-crystalline regions in clay systems. Soil Sci. Soc. Am. J., 35: 652–654.

Robin, M.J.L., Gillham, R.W. and Oscarson, D.W., 1987. Diffusion of strontium and chloride in compacted clay-based materials. Soil Sci. Soc. Am. J., 51: 1102–1108.

Shainberg, I., Alperovitch, N. and Keren, R., 1988. Effect of magnesium on the hydraulic conductivity of Na-smectite–sand mixtures. Clays Clay Miner., 36: 432–438.

Sharma, H.D. and Oscarson, D.W., 1991. Diffusion of plutonium in mixtures of bentonite and sand at pH 3. AECL, Chalk River, Ont., Rep. AECL-10435.

Sposito, G., 1984. The Surface Chemistry of Soils. Oxford University Press, New York, NY.

Whitworth, T.M. and Fritz, S.J., 1994. Electrolyte-induced solute permeability effects in compacted smectite membranes. Appl. Geochem. 9: 533–546.

Yong, R.N. and Warkentin, B.P., 1975. Soil Properties and Behaviour. Elsevier, Amsterdam.